

ARTICLE

# Several Theoretical and Applied Problems of Human Extreme Physiology: Mathematical Modeling

Grygoryan R.D.\*

Head of department “Human systems modeling”, Cybernetics Center; Institute of software systems of National Academy of Sciences, Kiev, Ukraine

---

ARTICLE INFO

*Article history*

Received: 6 December 2021

Accepted: 27 December 2021

Published: 30 December 2022

---

*Keywords:*

Cardiovascular system

Hemodynamics

Baroreflexes

Accelerations

Weightlessness

Simulation

---

ABSTRACT

Human cardiovascular system (CVS) and hemodynamics are critically sensitive to essential alterations of mechanical inertial forces in directions of head-legs (+Gz) or legs-head (-Gz). Typically, such alterations appear during piloting maneuvers of modern high maneuverable airspace vehicles (HMAV). The vulnerability of pilots or passengers of HMAV to these altering forces depends on their three main characteristics: amplitude, dynamics, and duration. Special protections, proposed to minimize this vulnerability, should be improved in parallel with the increasing of these hazardous characteristics of HMAVs. Empiric testing of novel protection methods and tools is both expensive and hazardous. Therefore computer simulations are encouraged. Autonomic software (AS) for simulating and theoretical investigating of the main dynamic responses of human CVS to altering Gz is developed. AS is based on a system of quantitative mathematical models (QMM) consisting of about 1300 differential and algebraic equations. QMM describes the dynamics of both CVS (the cardiac pump function, baroreceptor control of parameters of cardiovascular net presented by means of lumped parameter vascular compartments) and non-biological variables (inertial forces, and used protections). The main function of AS is to provide physiologist-researcher by visualizations of calculated additional data concerning characteristics of both external and internal environments under high sustained accelerations and short-time microgravity. Additionally, AS can be useful as an educational tool able to show both researchers and young pilots the main hemodynamic effects caused by accelerations and acute weightlessness with and without use of different protection tools and technics. In this case, AS does help users to optimize training process aimed to ensure optimal-like human tolerance to the altered physical environment. Main physiological events appearing under different scenarios of accelerations and microgravity have been tested.

## 1. Introduction

Already in the middle of XX-h century, under piloting of speed air flights it was revealed the fact that the human organism, during the long evolution adapted to earth

gravity conditions, is vulnerable to altered dynamic forces accompanying flight maneuvers<sup>[1]</sup>. Very soon experts realized that special protective technologies, capable of providing pilots' performances in the altered environment,

---

\*Corresponding Author:

Grygoryan R.D.,

Head of department “Human systems modeling”, Cybernetics Center; Institute of software systems of National Academy of Sciences, Kiev, Ukraine;

Email: [rgrygoryan@gmail.com](mailto:rgrygoryan@gmail.com)

have to be created and tested. Airspace flights, later provided by means of high maneuverable vehicles, deepened and widened the problem and identified a number of its additional and actual yet medical and technical aspects [2-10].

For a long time, the empiric way was the only one for searching, developing, and especially testing the every new protective algorithm or suit. This way has two immanent limitations - expensive and potentially hazardous for the human health and life. Therefore the alternative way based on computer simulations is encouraged [11-14]. Our consequential efforts in this direction resulted a special modified autonomic software (AS) for simulating and theoretical investigating of main dynamic responses of cardiovascular system (CVS) of a healthy person, armed by proper protections, to  $G_z$ -accelerations. AS is based on a system of quantitative mathematical models (QMM) consisting of about 1300 differential and algebraic equals.

The goal of this article is to introduce QMM, main characteristics of AS, and several simulations.

## 2. Basic Mathematical Models

Structurally and functionally, QMM is composed of two main blocks. The first - physiological block (PB) describes the physiology of CVS. The second - environmental block (EB) consists of models that describe both the dynamics of external physical forces and their investments in modulations of regional or global hemodynamics. Special part of EB imitates changes of extravascular pressures in cranial, pleural, and abdominal cavities, as well as in legs under voluntarily induced muscle stress and / or use of pneumatic protective suits. Here are also models for imitating the pilot's armchair and its position relative to the vector of accelerations.

PB includes three sub-models. The first sub-model describes the heart pump function (HPF) in quasi-static regimes of systemic and lungs blood flow. In fact, this model imitates continuous blood flows through both system and lung blood circles. The value of each flow is determined by the characteristics of appropriate (right or left) ventricles of the heart and by the venous pressures filling these ventricles. The second sub-model, based on the lumped parameter modeling technology [16-19], describes hemodynamics in a net of lumped parameter vascular compartments. At last, the third sub-model describes mechanisms based on both arterial mechanoreceptor reflexes and additional mechanisms of CNS controlling both the heart pump function and actual values of parameters of vascular compartments.

The model of HPF discloses main relationships between the mean for each cardiac cycle values of cardiac output

( $Q_i(t)$ ) and central venous pressure ( $P_{ai}^V(t)$  - for the right heart) or lung venous pressure ( $P_{a2}^V(t)$  - for the left heart). Additional factors that have been taken into consideration are the heart rate ( $F(t)$ ) and the inotropic coefficients ( $k_i(t)$ ) of the right or left ventricle, the hydraulic resistance ( $R_{avi}^K(t)$ ) of atria-ventricular valves, the duration of diastole ( $T_L(t)$ ), the diastolic elasticity ( $C_i(t)$ ), and the unstressed volume ( $U_i(t)$ ) of ventricles:

$$Q_i(t) = \frac{F(t) \cdot k_i(t) \cdot \left[ (\Delta P_{ai}^V(t) \cdot C_i(t) + U_i(t)) - U_{oi} \right] M_i(t)}{[1 - (1 - k_i(t))] M_i(t)}$$

$$M(t) = 1 - \exp\left(-\frac{T_L(t)}{R_{avi}^K \cdot C_i}\right),$$

$$P_{ai}^V(t) = P_i^{DNP}(t) + 0.735 \cdot \rho \cdot H_a^V(t) \cdot N^G \cdot \sin \phi(t) - P_i^{FD}(t),$$

$$T_L(t) = \frac{1}{F(t)} \cdot A + B \cdot (1 - k_i(t)),$$

$$P_i(t) = \begin{cases} 0, & V_i(t) < U_i(t) \\ (U_1(t) - U_i(t)) / C_i(t) & U_i(t) \leq V_i(t) \leq U_1(t) \\ (U_1(t) - U_i(t)) / C_i(t) + (V_i(t) - U_1(t)) / C_1(t) & V_i(t) > U_1(t) \end{cases},$$

$$V_i(t) = V_i(0) + \int_0^t (Q^I(t) - Q^O(t)) dt,$$

$$R_{av}^K(t) = \begin{cases} r_1, & \Delta P_K(t) > P_{KP}(t) \\ r_2, & \Delta P_K(t) \leq P_{KO}(t) \end{cases}$$

$$V^s(t) = \begin{cases} k_0 V^{ED}(t) - V_0(t), & P_v(t) \leq P_0 \\ k_1 V^{ED}(t) - V_1(t), & P_v(t) > P_0 \end{cases}$$

The low index  $i=1,2$  relates the value to the right heart or left heart chambers respectively.

The last formula is another reflection of the well-known regularity of HPF. This regularity is also known as the Frank-Starling's mechanism of HPF's self-control. It shows that relationships between stroke volume ( $V^s(t)$ ) of the ventricle and its end-diastolic volume may be presented as a linear approximation.  $C_i(t)$  and  $C_1(t)$  indicate the fact that dependences between pressures ( $P_i(t)$ ) and volumes ( $V_i(t)$ ), also known as  $P_i(V_i(t))$ -functions of heart chambers, are nonlinear. The nonlinearity plays an essential role during use of protections.

Our software consists of two version of the vascular net hemodynamics. In the frame of the first version (Figure 1), the vascular net is presented as 1-dimensional structure, consisting of  $j=33$  vascular arterial and venous compartments, each with its own fixed  $P_j(V_j(t))$  characteristics. These vascular compartments are located on the different levels relatively to the foot level. At the same time, they are completed into the several groups taking into account

common extravascular conditions in each of cavities or tissues. The atmospheric pressure is the extravascular pressure for the skin arterial and venous compartments.

In the second version of the CVS model, most regional vascular compartments are represented in form of a three-dimensional net. Compared with the scheme depicted in fig 1, in the three-dimensional net version, each compartment of legs vasculature, abdominal and thoracic vasculature have been tripled: each compartment has sub-compartments located below and above the median longitudinal Z-axis that conventionally represents the 0-level for two other additional perpendicular axes, namely, Y- axis (supine-chest) and X- axis (left hand-right hand). The three-dimensional net is necessary for the modeling and evaluating possible investments of blood re-distributions along of every perpendicular direction in the space-condition hemodynamics. The model helped us to better understand intimate mechanisms of specific hemodynamic shifts from the legs' area toward central and cranial basins, observed just after the engine of the space-vehicle stopped working and within the first several hours of the microgravity conditions. Such a model and simulations several results are described in [15,20].

In different arterial or venous vessels, biophysical pressure-volume characteristics (shortly presented as  $P_j(V_j(t))$ ) are essentially nonlinear and specific for each arterial or venous compartment. In the model, these nonlinear curves in j-th compartment of vessels are approximated by means of piecewise-linear characteristics, consisting of three parts. According to this approximation, a typical description of  $P_j(V_j(t))$  looks like:

$$P_j^T(t) = \begin{cases} (V_j(t) - U_j(t)) \cdot D_{0j}(t), & V_j(t) \leq U_j(t) \\ (V_j(t) - U_j(t)) \cdot D_{1j}(t), & U_j(t) \leq V_j(t) \leq U_{1j}(t) \\ ((U_{1j}(t) - U_j(t)) \cdot D_{2j}(t) + (V_j(t) - U_{1j}(t)) \cdot D_{1j}(t)), & V_j(t) > U_{1j}(t) \end{cases}$$

Here  $V_j(t)$  - is volume,  $U_j(t)$ ,  $U_{1j}(t)$  - are unstressed volumes, and  $D_{0j}(t)$ ,  $D_{1j}(t)$ ,  $D_{2j}(t)$  - represent the vascular total rigidity for different sections of the approximation,  $P_j^T(t)$  - is the local transmural pressure.

Blood flows between j-th and l-th vessel compartments, which are connected by means of hydraulic resistance  $R_{jl}(t)$ , are defined as a result of division of pressure gradients  $G_{jl}^P(t)$  by  $R_{jl}(t)$ . Transmural pressures  $P_j^T(t)$ , external pressures  $P_j^E(t)$ , and hydrostatic pressures  $P_{jl}^G(t)$  are considered as factors in determining  $G_{jl}^P(t)$ . Coefficients  $K_j^e(t)$ ,  $K_j^e(t)$  for  $P_j^E(t)$  or  $P_j^T(t)$  reflect differences in the levels of vessels' location and transmission characteristics of different tissues (muscles, cavities, skin) in which the vessel compartment is located:

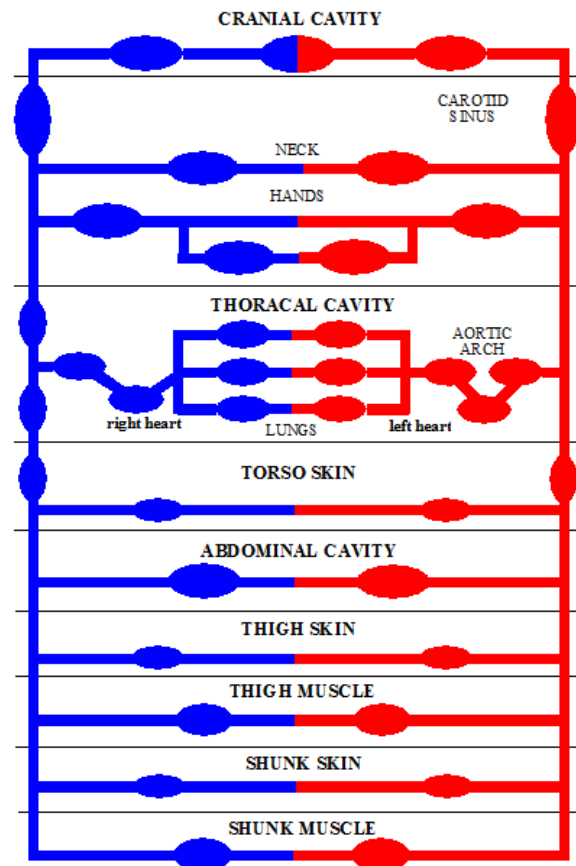


**Figure 1.** The first version of the lumped-parametric CVS model used for simulating of hemodynamic effects of so-called Gz-accelerations. Each compartment is located on its own distance from the foot-level.

$$q_{jl}(t) = \frac{G_{jl}^P(t)}{R_{jl}(t)}$$

$$G_{jl}^P(t) = (P_j^T(t) + K_j^e(t) \cdot P_j^E(t)) - (P_l^T(t) + K_l^e(t) \cdot P_l^E(t)) + P_{jl}^G(t)$$

$$P_{jl}^G(t) = N^G(t) \cdot \rho \cdot (L_j(t) - L_l(t))$$

The modeling of hemodynamic effects of acceleration is based on the calculation of every hydrostatic pressure as a function of both human posture and of the value of acceleration. We have two compartment level classes. The first one characterizes the value of distance between the human feet and the place of compartment's localization for human horizontal (clinostatic) or erect positions. The second class of levels (we call them real levels) reflects the value of hydrostatic pressures of human vessel compartments for person's all other positions. Using angle values between the horizontal and the directions of different body parts ( $\alpha$  - for calf,  $\beta$  - for thigh, and  $\gamma$  - for all other compartments of body and head vessels), these parameters can be calculated in the model according to the following formulae:

$$L^S = 0.5A \cdot l^S \cdot \sin \alpha,$$

$$L_1^t = (L_c - 0.5l_1^t \cdot \sin \beta) \cdot A,$$

$$L_2^t = L_1^t - 0.5A \cdot l_2^t \cdot \sin \beta,$$

$$L_p = L_c \cdot A,$$

$$L_{2i}^b = (l_{1i}^b - L_0) \cdot A \cdot \sin \gamma + L_0,$$

where  $l^S$ - length of calf,  $l_1^t, l_2^t$ - lengths of two parts of thigh,  $L_c$ - total length of legs,  $L^S$ - level of shank vessel compartment,  $L_1^t$  and  $L_2^t$ - real levels of thigh vessels compartments,  $L_p$ - level of aviation armchair seat place,  $L_0, l_{2j}^b, l_{1i}^b$ - real levels and initial lengths of localization for each j-th body or head vessel compartment.

Resistances of collapsible vessels have been calculated by means of special formulas:

$$R_1(t) = \begin{cases} R_0 \cdot \left(\frac{V_0}{V(t)}\right)^2, & P^T(t) > P_0 \\ R_0 \cdot r_0^4 \cdot \frac{a^2 + b^2}{2a^3 \cdot b^3}, & P_1 \leq P^T(t) \leq P_0 \\ R_1, & R_1 > R_0, P_1 < P_0 \end{cases}$$

$$a(t) = \frac{V(t) \cdot r_0^2}{V_0 \cdot b(t)}$$

$$b(t) = \frac{1}{3}r_0 \cdot \left[ d(t) + 2 \cdot \left(1 + \sqrt{1 - 2d^2(t) + d(t)}\right) \right]$$

$$d(t) = \frac{V(t)}{V_0}$$

$$R(t) = R_u \cdot \left(\frac{U(t)}{V(t)}\right)^2$$

$$V_0 = V(t)|_{p=0}$$

The total brain flow depends on changes (nervous origin) of the brain vascular resistance  $R^{AM}(t)$  that is modeled as:

$$R^{AM}(t) = \begin{cases} R_{min}^{AM}, & P^{AM}(t) \geq P_{max}^{AM}; \quad P_{min}^{AM} < P^{AM}(t) < P_{min}^C \\ R_{max}^{AM} \cdot C, & P_{max}^C < P^{AM}(t) < P_{max}^{AM} \\ \frac{E_1}{P^{AM}(t)}, & 0 \leq P^{AM}(t) \leq P_{min}^{AM} \end{cases},$$

where:

$$C = \left[ 1 - \exp\left(X_i \cdot \left(P^{AM}(t) - P_{max}^{AM}\right)\right) \right],$$

$$\frac{dR^{AM}(t)}{dt} = \frac{\delta_M \cdot P^{AM}(t) - R^{AM}(t)}{T_m}, \quad P_{min}^C < P^{AM}(t) < P_{max}^C.$$

$\delta_M$  is the time constant, and  $P^{AM}(t)$  is the pressure in cerebral arterioles.

In systemic veins, valves' resistance  $R_{jv}(t)$  is described as:

$$R_{jv}(t) = \begin{cases} R_{1j}, & q_j(t) > 0 \\ R_{2j}, & q_j(t) \leq 0, R_{1j} \gg R_{2j} \end{cases}$$

It is assumed that in the short observation intervals the total blood volume is stable:

$$\sum_i V_i(t) + \sum_j V_j(t) = \text{const.}$$

Dynamics of blood volumes in compartments are described by the following equation:

$$V_j(t) = V_j(0) + \int_0^t (q_j(t) - q_l(t)) dt$$

Three cavities (cranial, thoracic, and abdominal) are specially presented as extravascular environments that have their specific extravascular pressure dynamics. So, by such a presentation of vascular net, we are able to simulate important influences of extravascular pressures changes in these cavities on local hemodynamics. Having aortic arch and carotid sinus compartments, we are able to describe relationships between afferent nervous activity of mechanoreceptors (more exactly, in a multi-fiber afferent nerves) depending on local transmural pressures in these zones of baroreflex. However, before to describe formulas, useful is to explain our concept of the reflector control of hemodynamics under sustained and extreme amplitude Gz accelerations.

Baroreceptor reflexes caused from mechanoreceptors localized in aortic arch and carotid sinuses are well-known acute controllers of hemodynamics. This physiological view is mainly based on experiments, provided on anesthetized animals in their horizontal position. Indeed, in this position, mean pressures in aorta and carotid sinuses do not be essentially different. However, as it was demonstrated by means of mathematical modeling [18-21], already in head-up positions, carotid sinus receptors feel transmural pressure's lowering while receptors in the aortic arch may even be under slightly increased pressure. This compels these two reflexes, in clinostatics functioning in synergy manner, in altered positions to perform antagonism. Under +Gz accelerations [12-14,22], the antagonism becomes much severe and the depressor aortic baroreflex, trying

to lower the aortic pressure, does limit both the increase of heart rate and the increase of total vascular resistance. This suggests that high levels of the heart rate, observed during centrifuge tests or in real flight conditions, must have alternative providers. We think, mechanoreceptors of right atricus and those located in Willis circle can be these providers. In addition, the general pressor effects can be enhanced by nervous mechanisms associated with the activation of proprioceptors, humoral stressor factors, as well as with the critical lowering of total brain flow (this will cause general pressor response - GPR). According to this vision, the general structure of hemodynamics control under acceleration is presented in Figure 2.

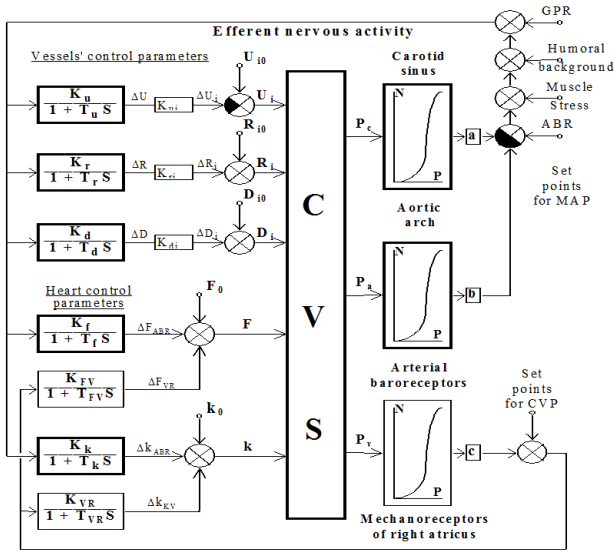


**Figure 2.** The general structure of hemodynamics' central nervous control model.

As it is shown in Figure 2, there are two heart control parameters ( $F, k$ ) and three integral control parameters of vessels ( $D, U, R$ ). The last three parameters are dispersed on different regional areas of vessels, according to the existing physiological notions about their efferent sympathetic nervous density.

Figure 2 consists of two different feedback channels. The first one in its turn forms two negative feedback channels for arterial baroreceptor reflexes (ABR) from baroreceptors of the aortic arch and the carotid sinus zones. The second feedback channel is a positive feedback channel for the mechanoreceptor reflex from the right atria area (this reflex is known as the Bainbridge reflex). The last one can only change  $F$  and  $k$ . The ABR is often included in different models of the hemodynamics' control but the Bainbridge reflex is rarely presented in models. In our model, the Bainbridge reflex is included by following reasons. The first reason is the essential increasing of central venous pressure during special breathing procedures.

The second reason is that the central venous pressure also increases during the muscle stress or use of extended coverage anti-G-trousers.

The nervous activity in both feedback channels is formed by the difference between the set-points in the central neuronal structures and the summary activity of receptors. ABR is presented in the model as independently functioning proportional regulators. They are based on local nonlinear S-form characteristics between arterial transmural pressures in aortic arch ( $q=1$ ), carotid sinus ( $q=2$ ) and brain arterioles ( $q=3$ ), from the one side, and their summary baroreceptor activity- from the other side. These characteristics take into consideration all known peculiarities of distinctions between threshold pressures and activity of baroreceptors:

$$N_q^R = \frac{1 - \exp\left(\beta_q^R \cdot (P_q^R - P_q^t)\right)}{1 + B_q \cdot \exp\left(P_q^R \cdot (P_q^R - P_q^t)\right)},$$

$$\frac{d\Delta X_i(t)}{dt} = \frac{K_i(t) \cdot E(t) - \Delta X_i(t)}{T_i},$$

$$K_i(t) = \begin{cases} K_i^p \cdot [X_i^{max} - X_i(t)] & E(t) > 0 \\ K_i^d \cdot [X_i(t) - X_i^{min}] & E(t) \leq 0 \end{cases}$$

$$X_i(t) = X_o + M_j^1 \cdot \Delta X_i(t),$$

$$E_q = P_q - p_q,$$

$$N_q^S = a \cdot N_q^R + c \cdot N_q^C,$$

$$X_i(t) = XB_i^{min} + \sum_{i=1}^n \Delta X_i(t),$$

$$T_q \frac{dN_q}{dt} = K_q \cdot N_q^S - N_q, \quad q = \overline{1, 3}.$$

Every central reflector control mechanism was simulated as a proportional regulator that has its stable gain ( $K_i$ ) and time constant ( $T_i$ ). Coefficients  $K_i$  characterize the power, whereas  $T_i$  characterize the values of inertia of reflector processes. We can simulate various conceivable hemodynamic situations by different combinations of changes in these parameters. It is necessary to note that there are some functional relations between  $K_i$  and control parameters ( $X_i$ ), namely,  $K_i$  decreases simultaneously with the increasing of  $X_i$ . Consequently, the functional reserves of CVS's control parameters have to decrease in parallel with the severity of loads.

In addition to the described model of CVS's own reflector mechanisms, and taking into account the well-

known physiologic concepts, our complex model includes also some assistant reflexes that might have outside origin (relative to the CVS structures). At the same time, we believe that by having some common tracks in brain structures, these assistant reflexes might influence the normal function of CVS's those own reflexes that are included in the model and essentially modify their hemodynamic effects.

According to this concept, we assume that there are three factors able to modify the arterial pressure's set-point level. They are:

- 1) Blood concentrations of cardio- and vasomotor active substances (especially catecholamines) -  $Y_{cat}$ ;
- 2) The general level of the body muscle activity -  $Y_m$ ;
- 3) The mentioned above general pressor reaction -  $Y_{GPR}$ .

Appropriate calculations have been provided with following formulas:

$$Y_{cat} = Y_{cat}^{max} \cdot \exp[-\omega \times (T - T_{exp})] / \{1 + \phi \cdot \exp[-\omega \cdot (T - T_{exp})]\}$$

$$Y_{gpr} = K_{gpr} \times Y \times \{1 - \exp[\eta \times (W_{gpr} - A)]\} / \{1 + \vartheta \times [1 - \exp[\eta \times (W_{gpr} - A)]]\}$$

$$Y_m = \theta \cdot P_m(t)$$

Formula for describing nonlinear dynamic effects of muscle pressure  $P_m(t)$  increasing under muscle stress is:

$$P_m(t) = [1 - \xi_p^h \cdot (h - 1)] \cdot [1 - \xi_j^p \cdot (j - 1)] \cdot \frac{1 - e^{-\theta^p [\theta_k^p - G(t)]}}{1 + \eta^p \cdot e^{-\theta^p [\theta_k^p - G(t)]}}$$

This formula takes into account possible changes in the dynamics of  $P_m(t)$  for male persons ( $j = 1$ ) or female persons ( $j = 2$ ), and also for the healthy ( $h = 1$ ) or weak ( $h = 0$ ) persons.

The next formula approximately presents the dependence between the value of the emotional stress  $S$  and acceleration. It includes sex-associated specifics and catecholamines' production / utilization differences depending on direction of acceleration's changes ( $\Delta g$ ):

$$S = \begin{cases} \gamma_m^s (1 - e^{-\alpha}) / (1 + \omega \cdot e^{-\alpha}), \Delta g > 0 \\ 3 \cdot \gamma_m^s (1 + \eta) \cdot (j - 1) \cdot e^{-\beta \cdot (r-t)} / (1 + \omega_1 \cdot e^{-\beta \cdot (r-t)}), \Delta g \leq 0 \end{cases} \quad \gamma_m^s = \overline{1,3}, (*)$$

This factor is modifying the coefficients of heart rate's baroreflexor control.

$$\Delta F^S = K_\gamma^F \cdot [1 + k_\gamma^F \cdot (j - 1)]$$

$$F_N = F_c \cdot [1 + k_j^F \cdot (j - 1) + \Delta F_S \cdot (1 + k_j^a \cdot a / a_0)] +$$

$$K_B^F (F^{\max} - F) \cdot C1 / (F^{\max} - F_{\min}) + \Delta F_B^B$$

It also will modify the general output of these control mechanisms as:

$$E_B = (1 + a_s \cdot S) \cdot Y_G^R - K_a^B \cdot N_a - K_c^B \cdot N_c - K_B^B \cdot N_B + K^m \cdot Y^m$$

Special notes on these modifications are described later in discussion section.

Three next formulas were chosen to additionally approximate changes in central nervous regulators causing by age ( $a$ ), sex ( $j$ ) and health ( $h$ ) factors.

$$E^I = N^R \cdot E_B \cdot (1 + \alpha^E \cdot a / a_0) \cdot [1 + f^E \cdot (j - 1)] \cdot [1 / (1 + K^h \cdot (h - 1))]$$

$$T^H = T_B^H \cdot (1 + K_h^H \cdot (h - 1)) \cdot [1 - f^H \cdot (j - 1)]$$

$$T^V = T_B^V \cdot (1 + K_h^V \cdot (h - 1)) \cdot [1 - f^V \cdot (j - 1)]$$

The actual formulas for calculating of vascular tonus characteristics (resistance  $r$ , rigidity  $d$  and unstressed volume  $U$ ) are followings:

$$r_n = r_n^B + K_n^r \cdot C^r \cdot C_0^V$$

$$d_n = d_n^B \cdot (1 + K_n^d \cdot C^d \cdot C_0^V)$$

$$U_n = U_n^B \cdot (1 - K_n^U \cdot C^U \cdot C_0^V),$$

where

$$C_0^V = \frac{V_s \cdot [1 - \xi \cdot (j - 1)] \cdot (1 + S)}{1 + \xi^h \cdot (h - 1)},$$

where

$$T \frac{dV_{ES}}{dt} = K_{ES} \cdot E^I - V_{ES}$$

In the last two mathematical expressions,  $S$  reflects emotional stress level,  $V_{ES}$  is the activity of efferent sympathetic nerves,  $E^I$  - is the output error in central contour of baroreflex.

So, the system of equations described above is the basic quantitative mathematical model capable to imitate responses of the human CVS and its physiological acute regulators to violations of the initial quasi-static values of both systemic and lung circulation. Although accelerations are the main cause of such violations, other factors like alterations of human pose, of local extravascular pressures, as well as changes of the background level of CNS' activity and / or concentrations of certain blood chemicals also can be initiators of hemodynamic violations. Regulator mechanisms presented in the model are activating against these initial violations.

The approximate numerical solution of the system of model equations is carried out by the Euler method. Previously, the model constants were tuned in a way that ensured a good accordance of simulation data with empirical data known for three postures (horizontal, head-up, and head-down) of the healthy human, as well as under several well-studied additional tests. The final version of software provides special algorithms for calculations of the model in accordance with the actual acceleration profile. Calculations also can be interrupted under appearance of two special cases. The first one is if the systolic pressure in ar-

terioles of eyes is less than the level sufficient for providing pilot's vision. The second one is when the total brain flow is critically low to provide pilot's consciousness. In both cases, calculations interruption is accompanied with proper information about cause of the break. After the calculations have been made, their results appear in graph forms.

### 3. Several Results of Simulated Accelerations

There were created model versions approximately adapted to the person's age, sex, body mass, and height. All adaptation procedures use the basic model to automatically calculate characteristics of vascular compartments in order to provide initial steady-state hemodynamics. Adaptation algorithms and software use initial quantitative data given for cardiovascular characteristics of the mean healthy man of mass 70 kg and height 170 cm. So, the total blood volume is 5200 cm<sup>3</sup>.

Special physiologist oriented user interface (UI), providing both preparations and execution of the computer experiment (in other words - simulation), was created. The screen-forms in Figure 3 illustrates the main opportunities provided by the UI for a scenario constructing for the current computer experiment (simulation). The user can choose one of four options to actualize model parameters, acceleration profile, protections, as well as certain additional options, necessary for the analysis of simulation results, provided as graphs. Namely, the picture below concerns means of protections and their actual parameters. It is shown that the experiment will be provided for the case when all four protections (stressing of muscles, breathing under positive pressures, three-sectional pneumatic suit, and the seat-angles of the pilot armchair) are activated at the time moment, when Gz accelerations overcame the threshold level of 2 g/sec.

Figures 4 and 5 represent both the used acceleration profile (bottom part) and certain hemodynamic variables under trapezoidal acceleration profile.

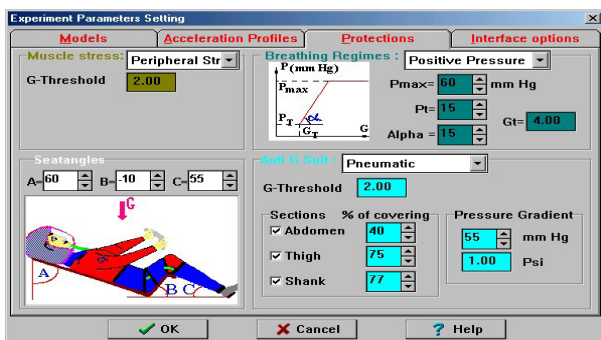


**Figure 3.** The screen-form of the user interface (UI) for setting actual characteristics of protections.

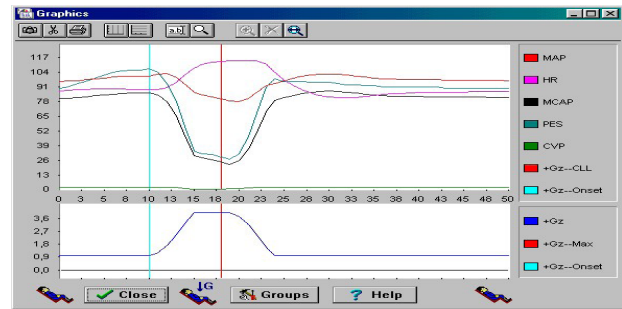


**Figure 4.** The dynamics of mean arterial pressure (MAP), mean pressure in carotid sinus (MCAP), systolic arterial pressure on the eye level (PES), central venous pressure (CVP) and heart rate (HR) under trapezoid profile accelerations with the acceleration and deceleration gradients 1g/s (the bottom part of the figure). The mean relaxed man. The emotional stress regime is set on moderate position. Seat back angle = 12°.

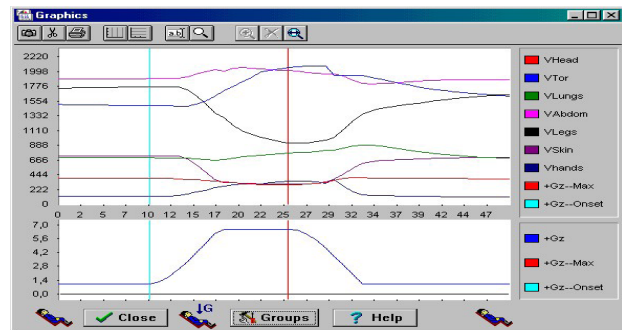


**Figure 5.** The dynamics of blood volumes in different body sections (Vtor - thorax; Vabdom - abdominal; VLungs - lungs; Vlegs- legs; Vhead - head; Vhand -Hands; Vskin - Skin) under trapezoid profile accelerations with the acceleration and deceleration gradients 1g/s (the bottom part of the figure). The mean relaxed man with use of pneumatic anti-G suit. The suit is pressured with gradient 1.5 Psi after the acceleration exceeds 2 g. Sections' covering percents are the following: abdominal -35%; thigh -75%; shank - 90%. The emotional stress regime is set on moderate position. Seat back angle = 30°.

In contrast, Figure 6 illustrates the case of a steeper acceleration increase and decrease profile under pilot's natural breathing.

The dynamics of mean arterial pressure (MAP), mean pressure in carotid sinus (MCAP), systolic arterial pressure on the eye level (PES), central venous pressure (CVP) and heart rate (HR) under trapezoid profile accelerations with the acceleration and deceleration gradients 1g/s (the bottom part of the figure). The mean relaxed man. The emotional stress regime is set on moderate position. Seat back angle = 30°.

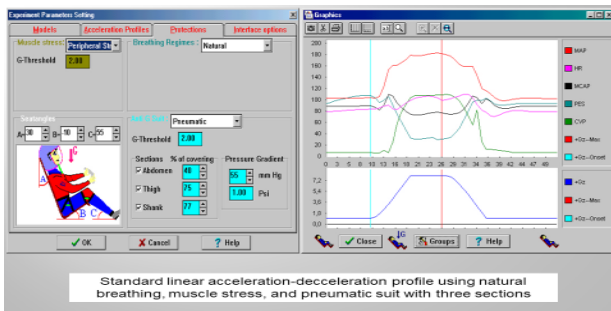


Figure 6. Parameters of used protections (left-side) and simulation results (right-side).

back angle = 30°.

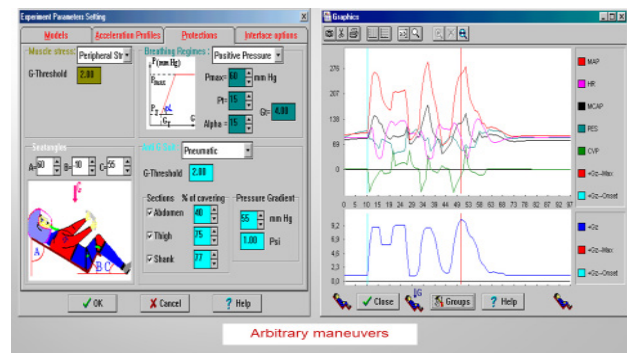


Figure 9. Parameters of used protections (left-side) and simulation results (right-side).

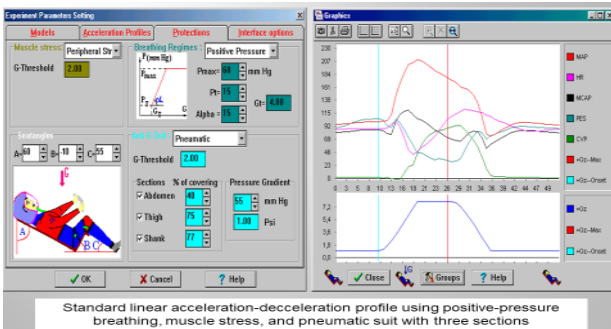


Figure 7. Parameters of used protections (left-side) and simulation results (right-side).

The dynamics of mean arterial pressure (MAP), mean pressure in carotid sinus (MCAP), systolic arterial pressure on the eye level (PES), central venous pressure (CVP) and heart rate (HR) under arbitrary profile accelerations with the acceleration and deceleration gradients 2 g/s (the bottom part of the figure). The stressed man. The emotional stress regime is set on the top position. Seat back angle = 60°.

The dynamics of mean arterial pressure (MAP), mean pressure in carotid sinus (MCAP), systolic arterial pressure on the eye level (PES), central venous pressure (CVP) and heart rate (HR) under trapezoid profile accelerations with the acceleration and deceleration gradients 1g/s (the bottom part of the figure). The mean relaxed man. The emotional stress regime is set on moderate position. Seat back angle = 60°.

#### 4. Acute Alterations of Hemodynamics under Weightlessness: Special Role of Diaphragm Biomechanics in Pleural Pressure

Accelerations at the stage of placing a manned spacecraft into orbit, as well as the transition from the active phase to orbital flight, are accompanied by a number of biomechanical and physiological processes that have not been yet clearly understood and estimated. The proper organization of both pre-flight training and the prevention of the adverse effect of microgravity on the organism are important for providing of astronauts performance and health after returning to Earth. However, namely initial processes during the transition to weightlessness condition are still largely unclear. Among the controversial issues, the direction and magnitude of changes in central venous pressure play a key role for hemodynamics. Until the late 1980s, the dominant view was that CVP grows due to blood redistribution from the legs and abdominal cavity to the thoracic and cranial basins. Moreover, direct measurements of CVP in zero gravity were not carried out. The reasoning was based on the puffiness of the neck and faces, as well as on the phenomena known as "bird legs", the appearance of the waist, as well as the expansion of the girth of the chest segment of the astronaut's body. Almost all of these phenomena were well reproduced in terrestrial conditions using an antiorthostatic (head-down) posture with an inclination angle of -4 deg. up to -12 deg. It was

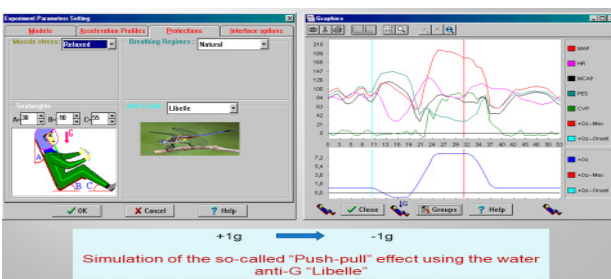


Figure 8. Parameters of used protections (left-side) and simulation results (right-side).

The dynamics of mean arterial pressure (MAP), mean pressure in carotid sinus (MCAP), systolic arterial pressure on the eye level (PES), central venous pressure (CVP) and heart rate (HR) under trapezoid profile accelerations with the acceleration and deceleration gradients 1g/s (the bottom part of the figure). The mean relaxed man. The emotional stress regime is set on moderate position. Seat

in accordance with this concept that prevention procedures and algorithms were developed. However, nausea and deterioration in the well-being of astronauts in the acute period of adaptation to microgravity urgently required the development of more effective countermeasures. Therefore, the search for more adequate methods for modeling the primary phase of human adaptation in weightlessness was an important task of space medicine.

Mathematical modeling has become one of the alternative methods. Below are the results of such a simulation. However, before considering them in detail, I would like to dwell on one biomechanical aspect of this problem, namely, the possible role of pressure in the pleural cavity in the changes observed in real space flight.

The long-term adaptation of animal and human life to the conditions on Earth has led to close associations between respiration and blood circulation. Inhalation is carried out due to the combined changes in the activities of the intercostal muscles and the diaphragm. Moreover, exhalation is a largely passive process that occurs due to the return of the chest to its original state (under the influence of weight). It is important that the outer pleura sheet is mechanically attached to the muscles of the chest cavity and to the diaphragm. Thus, the moving of the diaphragm into the abdominal cavity and the expansion of the chest cavity are two independent factors that deepen the level of initially sub-atmospheric pressure in the closed pleural cavity. A drop in pleural pressure expands the lungs and inhalation occurs, while an increase in pleural pressure leads to exhalation. This normal biomechanics of respiration also affects the CVP: during the phase of inhalation, the CVP decreases, and during the phase of exhalation, on the contrary, the CVP increases. These changes in the CVP modulate venous return both in the superior and in the inferior vena cava. So, total blood volumes in cranial basin and in body lower part are negatively correlating with the dynamic of CVP.

Now let us turn attention to Figure 10.

Numbers in the right-side picture indicate: 1- lungs; 2- the heart; 3- the diaphragm; 4- abdominal organs. Three color rectangles symbolize the fact that the descending aorta, the inferior vena cava; and the esophagus, piercing through the diaphragm, mechanically connect the latter with organs of thoracic and abdominal cavities. The left-side picture schematically illustrates relative effects of different inertial forces on the diaphragm position.

The right-side picture schematically illustrates certain anatomical details of thoracic and abdominal organs. Important is that the descending aorta (red rectangle), the inferior vena cava (blue rectangle), and the esophagus (yellow rectangle), that is piercing through the diaphragm

thus mechanically connect the latter with organs of thoracic and abdominal cavities. In Earth conditions, because of abdominal organs weight, the diaphragm position does depend on human postures. Moreover, the diaphragm position is associated with the direction and magnitude of mechanical forces, altering under accelerations or weightlessness (left-side picture). Namely, these facts were used for creating and consistent improvement of adequate mathematical model of human hemodynamics under altering gravitational forces <sup>[15,20,21]</sup>.

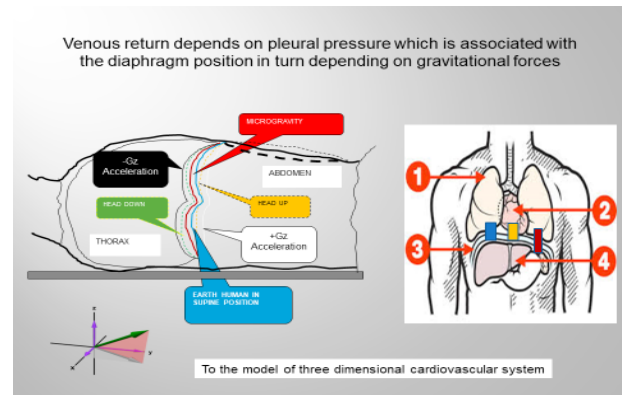


**Figure 10.** Schematic illustration of relationships between gravity induced mechanical forces and diaphragm position that were taken into account under modeling of hemodynamics in a three-dimensional vascular net.

Partial simulation results concerning blood distributions both in human body segments and in the frame of every segmental levels (back, axis, and chest) are collected in the table.

Data in the table are collected in two groups of columns. The first group, located in the left side, represents four columns of data generally concerned with simulations of four body positions; the rest condition on a back; the head up position of 90 deg.; the head down condition of 90 deg.; and the special head down posture of 6 deg. We can state that the simulated total sectional blood volumes shown in the table are very close to analogous empirical data. This was a reason to start simulate processes appearing in CVS just after the spaceship's engine stops to work. Appropriate simulation data are collected in four right-side columns. Special should be noted that the column, concerned with the engine stopping, presents data simulated under supposing the person has certain emotional stress.

Next four columns collect simulated data for two hypotheses. The first hypothesis is that the microgravity affects only the CVS function. Appropriate volumes present the simulations only for two time moments of weightlessness: in its 30-h seconds and 3-d min. For each time mo-

**Table 1.** Simulated blood volumes in body sections and their three layers (chest, axis, and back) under Earth gravity and microgravity conditions.

		Body positions (Earth gravity)				Engine stop	Microgravity (hypotheses)				
		Horizontal on back	Head up 90 deg.	Head down 90 deg.	Head down 6 deg.	Logement position + 3Gz	HO 30 s	HO 3 min	HI 30 s	HI 3 min	
BLOOD VOLUMES ( ml) IN BODY SECTIONS	Head	Total	415	333	597	431	350	433	423	438	429
		Chest	135	111	166	141	113	144	141	146	143
		Axis	139	111	166	144	117	144	141	146	143
		Back	141	111	166	146	120	144	141	146	143
	Neck	Total	143	90	289	152	95	152	147	157	143
		Chest	35	21	51	39	21	40	39	42	41
		Axis	68	47	85	71	50	72	69	74	71
		Back	40	21	2	42	24	40	39	42	41
	Thoracic	Total	1870	1575	2490	1990	1620	1915	1890	1620	1540
		Chest	435	388	650	478	340	490	485	390	368
		Axis	820	795	1180	970	810	940	915	845	805
		Back	510	388	650	538	468	490	485	390	368
	Abdominal	Total	1080	1230	1050	1147	1325	1005	1054	1245	1347
		Chest	323	406	357	348	430	332	355	414	446
		Axis	347	415	225	365	445	340	355	419	446
		Back	410	406	357	438	449	332	355	414	446
	Hips	Total	816	983	333	498	895	810	810	835	842
		Chest	245	328	111	183	289	270	270	278	280
		Axis	276	328	111	222	296	270	270	278	280
		Back	295	328	111	394	310	270	270	278	280
	Shins + Foals	Total	520	602	310	415	546	509	508	519	521
		Chest	165	201	103	136	181	170	169	173	174
		Axis	174	201	103	138	182	170	169	173	174
		Back	177	201	103	141	184	170	169	173	174
	Hands	Total	326	351	384	327	337	338	330	345	339

ment, two hypotheses have been simulated. In the frame of the hypothese0 (in the table denoted “H0”), the only hemodynamic influence is caused by the loss of the blood hydrostatic pressure. The hypothese1 (in the table denoted “H1”) supposes additional changes, namely, increase of pleural pressure on 12 mm Hg and decrease of extravascular pressure in abdominal cavity on 6 mm Hg.

As one can see, the simulated cranial hypervolemia accompanied by decreases of blood volumes in legs and abdomen area is fixed. Namely, such a general picture of hemodynamic shifts have had been observed during the real cosmic flights [4,5,8-10].

### 5. Discussion

Two fundamental problems covering multiple aspects of human physiology in extreme environmental conditions have been analyzed using non-traditional approach based on quantitative mathematical models and computer simulations. Earth gravity is the consistent environmental

factor evolutionarily determined structural-functional aspects of human body anatomy and physiology. Adaptation boundaries were mainly concerned with loads associated with postural changes. As modern airspace flights revealed, these boundaries are not sufficient for providing human health and performance under sustained acceleration and / or microgravity [1-9,23-26]. Mathematical modeling and computer simulations have been recognized by physiologists-empiricists as prospective assistant research tool, making the process of research and development of protective technologies both less dangerous and cost-effective [27-31]. However, it is important to take into account a huge number of physiological mechanisms, facts, and observations capable help to disclose real acting forces accompanying modern airspace flights. A particular but not less important problem is models verification. As a rule, empiricists have not the complete measurements necessary for models verification. The only way to get out of the existing impasse, use heuristics based both on

the experience of creating simpler models and on testing models in those situations that are most studied. But even the indicated paths do not guarantee the correctness of the simulation results. Therefore, the conclusions that follow from the simulations are subject to empirical verification. Our experience in modeling of various physiological systems and mechanisms allows us to hope that the results presented in the article will meet the due interest of traditional physiologists.

Computer simulations on the model of a three-dimensional cardiovascular system has shown that the slight elevation of the pleural pressure is the most likely mechanism impeding venous return from the cranial basin [6]. Simulations gave arguments for proposing the following conceptual scheme of alterations in hemodynamics under short-time microgravity.

As to modeling of hemodynamic effects of positive (+Gz) or negative (-Gz) accelerations, it is useful to provide some additional arguments for the adequacy of the models. First of all, our models have a long prehistory. The basic models were developed and properly verified for simulating human cardiovascular responses to postur-

al tests [18]. The next phase of models modernization was their augmentation for simulating slow (about 0.1 g/sec) increasing moderate (up to 3 g) +Gz accelerations without use of protection suits [12]. Step-by-step, new physiological mechanisms and protective technologies were added, tuned, and tested. As a result, a simulator "PILACCEL" was successfully created and tested using data presented by experts of the Laboratory of Biodynamics (chief at that time - Dr. William Albery) in Wright Patterson Air Force Base USA [13,14]. After that time, both models and software were modified [19,14]. These modifications of models were based on data presented in [33-36]. Results, presented in this article, have been obtained by means of the advanced software.

Experts know that the top value of human tolerance to standardized profile of +Gz acceleration loading may have essential variability. The variability is characteristic both during results comparison observed on different subjects and even in frame of different observations for one subject. Factors determining this variability were analyzed to include them in our models. Such approach will help one both to understand why the published results of different

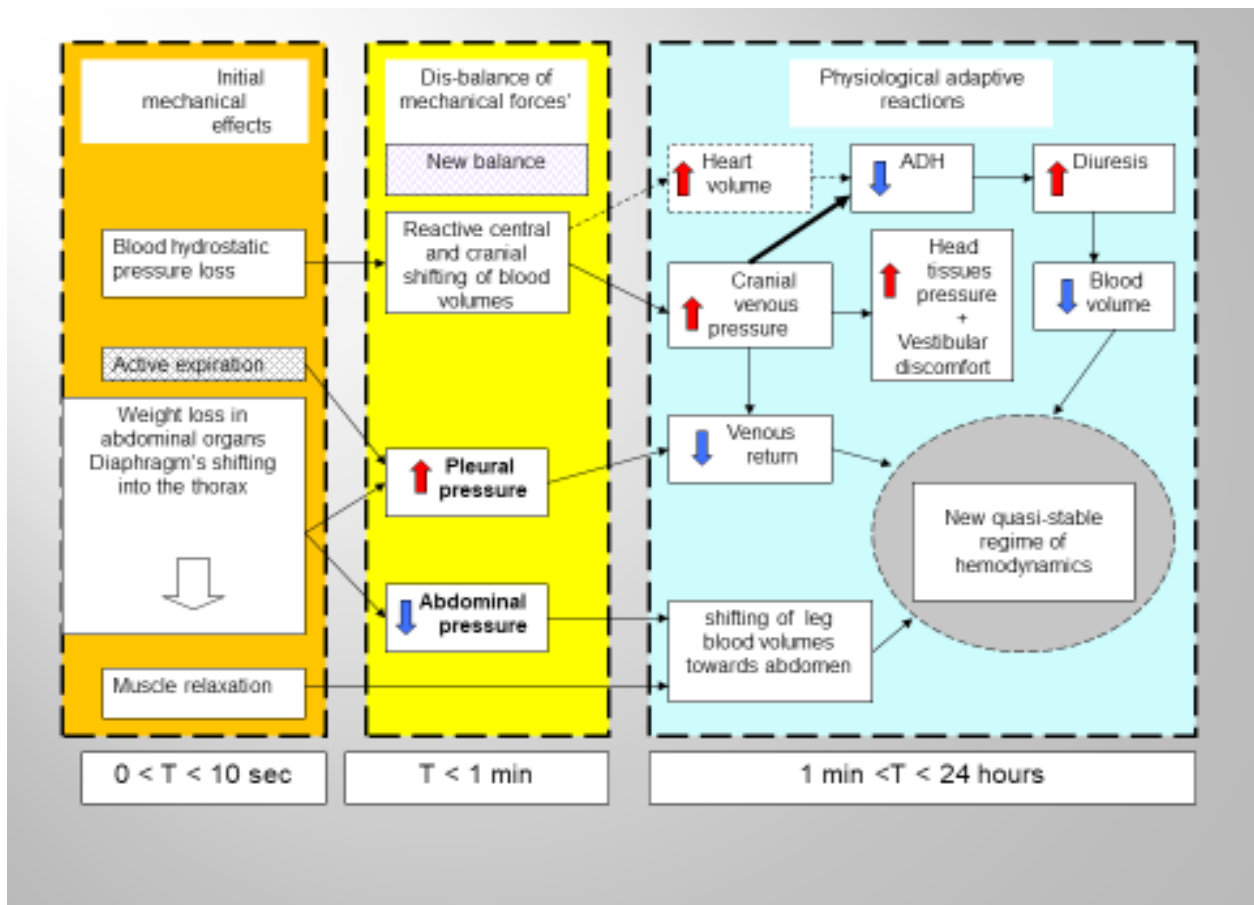


Figure 11. Conceptual scheme of alterations in hemodynamics under short-time microgravity.

investigators have a wide disperse, and how to effectively use our models. This analysis is also aimed to determine an acceptable approach to the problem, how to optimize protections use.

Generally speaking, all anthropologic, psychological, physiological and environmental factors that theoretically may influence on the top limit of human tolerance to +Gz acceleration may be divided into two different groups, containing observable and non-observable factors. Let's the factors that potentially might be controlled by investigator, consider here as the first factors group. Into the factors' second group we include the factors that may be considered as causal within every observation. So, this vision platform lets us to imagine that the variability between every two observations is sooner a regular event than an exclusive one. An additional useful condition for our analysis is the assumption that among the factors of the first group we also can mark two subgroups according to the factor's relative role in providing of human tolerance to Gz acceleration. The list of the major factors determining top value of the tolerance consists of several anthropometric, psychological, physiological and environmental characteristics. Perhaps, in the most advanced model, these characteristics should have been considered input parameters too.

Special notes concerning emotional stress under extreme accelerations (see formula (\*)) could help the reader to better imagine both the necessity and the technology of simulation. In our initial model of moderate accelerations<sup>[12]</sup>, values of regulators' gains had been the same that was argued for the model created to simulate human hemodynamics under postural tests<sup>[18]</sup>. However, trying to simulate extreme accelerations, we meet a problem - responses of the heart rate were essentially lower than empirical results. In addition, the simulated loss of vision appeared earlier than it was known for centrifuge tests. I have had consulted on this subject with well-known experts (professors Russell Burton and Ulf Balldin). They recommended to pay attention on the fact that blood tests just after sustained centrifuge accelerations have shown essential elevations of blood catecholamines compared with the rest conditions before centrifuge onset. Namely, approximation formula (\*) was chosen in assumption that accelerations a priori increase the concentration of blood catecholamines. Approximation parameters in (\*) were chosen in order to have acceptable adequacy of simulated and empirical observations for heart rate and the time of loss of peripheral vision.

Concerning microgravity conditions, some thoughts can be added. In ground conditions, the weight of the organs of the chest cavity, in particular - of the abdominal

cavity - is an independent modulator of the shape and tension of the diaphragmatic muscle. Therefore, this weight plays a significant role in forming of the pleural pressure. Just before the transition to orbital flight, the diaphragm of the astronaut, experiencing about 3 units of +Gz accelerations, is both tensed and maximally displaced into the abdominal cavity. So, the pleural cavity is increased thus the pleural pressure is minimal. As soon as the ship's engines cease to create thrust, the weight of the internal organs disappears, and the muscular tension of the diaphragm removes it into the chest cavity until a balance of mechanical forces acting on the diaphragm from its both sides is achieved.

The key to this transformation is that the pressure in the pleural cavity rises. But this rise in real conditions has one more reason - exhalation in weightlessness can only be active, i.e. the intercostal respiratory muscles contract and press on the pleura. Thus, venous return in zero gravity will be difficult, which will lead to accumulation of blood in the cranial basin and in the vessels of the lower body. It remains to explain why the blood in the lower part of the astronauts decreases in flight.

In my opinion, the explanation is related to two nuances. First, due to the fact that the adaptation of a bipedal person to Earth's gravity was aimed at preventing the collapse of cerebral circulation, a natural asymmetry of the innervation of the arterioles of the lower and upper parts of the body has developed. The density of the innervation of the arterioles of the abdominal cavity and legs is much greater than the density of the innervation of the vessels of the upper body. Secondly, arterial mechanoreceptors respond to the value of transmural pressure, which will be the lower, the higher the extravascular (specifically, pleural) pressure is. Consequently, reflex reactions developing in conditions of short-term weightlessness will contribute to a greater narrowing of the arterioles of the lower part of the body and a decrease in the volume of blood in them. In this case, the outflow of blood from the vessels of the cranial basin is still difficult. A gradual decrease in these symptoms is the result of increased urine output, which is most likely caused by stretch receptors in the cerebral sinuses.

## 6. Conclusions

Human hemodynamics is critically sensitive both to essential alterations of mechanical inertial forces in directions of head-legs (+Gz) or legs-head (-Gz) and to microgravity condition. Typically, such alterations appear during pilotage maneuvers of modern high maneuverable airspace vehicles (HMAV). Pilots' or passengers' vulnerability to these altering forces depends on force's

three main characteristics: amplitude, dynamics and duration. Special protections, proposed for minimizing of the vulnerability, should be improved in parallel with the increasing of these hazardous characteristics of HMAVs. As the empiric testing of novel protection methods and tools is both expensive and hazardous, computer simulations are encouraged. Autonomic software (AS) for simulating and theoretical investigating the main dynamic responses of human cardiovascular system (CVS) to altering gravitational forces is developed. AS is based on a system of quantitative mathematical models (QMM) consisting of about 1300 differential and algebraic equals. QMM describes the dynamics of both CVS (the cardiac pump function, baroreceptor control of parameters of cardiovascular net presented by means of lumped parameter vascular compartments) and non-biological variables (inertial forces and used protections). The main function of AS is to provide physiologist-researcher by visualizations of calculated additional data concerning external and internal environments under high sustained accelerations and short-time microgravity. Additionally, AS can be useful as an educational tool able to show both researchers and young pilots the main hemodynamic effects caused by accelerations and acute weightlessness with and without use of different protection tools and technics. In this case, AS does help users to optimize training process aimed to ensure optimal-like human tolerance to the altered environment. Main physiological events appearing under different scenarios of accelerations and microgravity have been tested.

It is worth to underlie that simulations have shown principally new phenomenon. Namely, extreme Gz accelerations are special environmental factor capable of transforming the normally synergic functions of aortic arch and carotid sinuses baroreflexes to their antagonistically functioning. This publication reveals some intimate aspects of the modeling that were not reflected in models analyzed in <sup>[37]</sup>. The modeling is also approachable for the deeper understanding of other physiological mechanisms responsible both for the normal and for the several pathological functioning of CVS. In the next publication, I would like to present models and simulations, concerned with the much more complex physiology of mechanisms that are responsible for acute, middle-time and long-time neural-humoral control of human circulation.

## References

- [1] Morgan, T.R., 10 October 2000. Physiology of G Exposure & Protection. AFRL.
- [2] Scott, J.M., Esch, B.T., Goodman, L.S., et al., 2007. Cardiovascular consequences of high-performance aircraft maneuvers: implications for effective countermeasures and laboratory-based simulations. *Appl. Physiol. Nutr. Metab.* 32, 332-339. DOI: <https://doi.org/10.1139/h06-087>.
- [3] Lawley, J.S., Petersen, L.G., Howden, E.J., et al., 2017. Effect of gravity and microgravity on intracranial pressure. *J. Physiol.* 595, 2115-2127. DOI: <https://doi.org/10.1113/JP273557>.
- [4] Nicogossian, A.E., Williams, R.S., Huntoon, C.L., et al., 2016. *Space Physiology and Medicine: from Evidence to Practice*. Springer.
- [5] Tanaka, K., Nishimura, N., Kawai, Y., 2017. Adaptation to microgravity, deconditioning, and countermeasures. *J Physiol Sci.* 67, 271-281. DOI: <https://doi.org/10.1007/s12576-016-0514-8>.
- [6] Mandsager, K.T., Robertson, D., Diedrich, A., 2016. The function of the autonomic nervous system during spaceflight. *Clin. Auton. Res.* 25, 141-151. DOI: <https://doi.org/10.1007/s10286-015-0285-y>.
- [7] Watenpaugh, D.E., 2016. Analogs of microgravity: head-down tilt and water immersion. *J. Appl. Physiol.* 120, 904-914. DOI: <https://doi.org/10.1152/japplphysiol.00986.2015>.
- [8] Zhang, L.F., Hargens, A.R., 2018. Spaceflight-induced intracranial hypertension and visual impairment: pathophysiology and countermeasures. *Physiol. Rev.* 98, 59-87. DOI: <https://doi.org/10.1152/physrev.00017.2016>.
- [9] Goswami, N., White, O., Blaber, A., Evans, I., et al., 2021. Human physiology adaptation to altered gravity environments. *Acta Astronautica.* 189, 216-221. DOI: <https://doi.org/10.1016/j.actaastro.2021.08.023>.
- [10] Demontis, G.C., Germani, M.M., Caiani, E.G., et al., 2017. Human Pathophysiological Adaptations to the Space Environment. *Front. Physiol.* 02. DOI: <https://doi.org/10.3389/fphys.2017.00547>.
- [11] Melchior, F.M., Srinivasan, R.S., Ossard, G., Clère, J.M., 1993. A mathematical model of the cardiovascular response to +Gz acceleration. *Physiologist.* 36(1 Suppl), S62-3. PMID: 11537428.
- [12] Grygoryan, R.D., Kochetenko, E.M., 1996. Informational technology for modeling of fighters medical testing procedures by centrifuge accelerations. *Selection & Training Advances in Aviation: AGARD Conference Proceedings 588; Prague, May 25-31, PP3, 1-12.*
- [13] Grygoryan, R.D., 1999. Development of a hemodynamics computer model of human tolerance to high sustained acceleration exposures. *EOARD Contract NoF61708-97-W0253: Final Report.* pp. 62.

- [14] Grygoryan, R.D., 2002. High sustained G-tolerance model development. STCU#P-078 EOARD# 01-8001 Agreement: Final Report. pp. 66.
- [15] Grygoryan, R.D., Hargens, A.R., 2008. A virtual multicellular organism with homeostatic and adaptive properties. In: *Adaptation Biology and Medicine: Health Potentials*. Ed. L. Lukyanova, N. Takeda, P.K. Singal. - New Delhi: Narosa Publishing House. 5, 261-282.
- [16] Kokalari, I., 2013. Review on lumped parameter method for modeling the blood flow in systemic arteries. *Journal of Biomedical Science and Engineering*. 06(01), 92-99.  
DOI: <https://doi.org/10.4236/jbise.2013.61012>.
- [17] Shimizu, S., Une, D., Kawada, T., Hayama, Y., Kamiya, A., Shishido, T., Sugimachi, T., 2018. Lumped parameter model for hemodynamic simulation of congenital heart diseases *The Journal of Physiological Sciences*. 68, 103-111.  
DOI: <https://doi.org/10.1007/s12576-017-0585-1>.
- [18] Grigorian, R.D., 1983. Hemodynamics' control under postural changes (mathematical modeling and experimental study). Ph.D thesis. Kiev: Institute of Cybernetics. pp. 214. (in Russian).
- [19] Grygoryan, R.D., 2017. Problem-oriented computer simulators for solving theoretical and applied tasks of human physiology. *Problems in programming*. 3, 161-171.  
DOI: <https://doi.org/10.15407/pp2017.03.161>.
- [20] Grigorian, R.D., 1990. Modeling the interactions of mechanoreflexes in the zones of high and low pressure. *Cybernetics and Computing technology*, N.Y. Allerton press. 314, 745-748.
- [21] Grigoryan, R.D., 1986. Three-dimensional mathematical model of human hemodynamics", *Cybernetics and Computing Tecnology*, N.Y. No.70, pp. 54-58.
- [22] Grigoryan, R.D., 1987. A theoretical analysis of some physiological mechanisms of human tolerance to +Gz accelerations, *Space Biol. and Airspace Med.* (in Russian). 5, 95- 96.
- [23] Convertino, V., Hoffler, G.W., 1992. Cardiovascular physiology. Effects of microgravity. *J Fla Med Assoc*. 79(8), 517-524.
- [24] Hargens, A.R., Watenpaugh, D.E., 1996. Cardiovascular adaptation to spaceflight. *Med Sci Sports Exerc*. 28(8), 977-982.
- [25] Buckley, J.C.Jr., Gaffney, F.A., Lane, L.D., et al, 1996. Central venous pressure in space. *J Appl Physiol*. 81(1), 19-25.
- [26] Burton, R.R., Smith, A.H., 1996. Adaptation to acceleration environments. Capt. 40 In: *Environmental physiology*. Vol.II Eds. M.J. Fregly and C.M. Blatteis. Oxford Univ.Press. 943-1112.
- [27] Jaron, D., Moore, T.W., 1984. A cardiovascular model for studying impairment of cerebral function during +Gz stress. *Aviat., Space Environ.Med*. 55, 24-31.
- [28] Burton, R.R., 1998. Mathematical models for predicting straining G-level tolerances in reclined subjects. *J.Grav.Physiol*.
- [29] Cirovic, S., Walsh, C.D., Fraser, W.D., 2000. A mathematical model of cerebral perfusion subjected to Gz acceleration. *Aviation Space and Environmental Medicine*. 71(5), 514-521.
- [30] Yang, C., Sun, X., Geng, J., Wang, Y., Zhou, Y., Wang, P., 2007. Study on the changes of heart rate during "push-pull effect" simulation using a tilt table combined with a lower body negative pressure device. *Chin. J. Aerospace Med*. 18, 171-175.  
DOI: <https://doi.org/10.3760/cma.j.issn.1007-6239.2007.03.003>.
- [31] Grygoryan, R.D., Lissov, P.N., Aksenova, T.V., Moroz, A.G., 2009. Specialized software-modeling complex "PhysiolResp". *Problems in programming*. 2, 140-150.
- [32] Grygoryan, R.D., Lissov, P.N., 2004. A software simulator of human cardiovascular system based on its mathematical model. *Problems in programming*. 4, 100-111.
- [33] Goodman, L.S., Banks, R.D., Grissett, J.D., Saunders, P.L., 2000. Heart rate and blood pressure responses to +Gz following varied-duration -Gz. *Aviat. Space Environ. Med*. 71, 137-141.
- [34] Balldin, U.I., Derefeldt, G., Eriksson, L., et al., 2003. Color vision with rapid-onset acceleration. *Aviat. Space Environ. Med*. 74, 29-36.
- [35] Hakeman, A.L., Shepard, J.L., Sheriff, D.D., 2003. Augmentation of the push-pull effect by terminal aortic occlusion during head-down tilt. *J. Appl. Physiol*. 95, 159-166.  
DOI: <https://doi.org/10.1152/japplphysiol.01079.2002>.
- [36] Yang, C., 2007. Study of simulation method and protection training of push-pull effect. Ph. D. thesis. Xi'an: Fourth Military Medical University.
- [37] Grygoryan, R.D., 2020. Milestones of the modeling of human physiology. *Journal of Human Physiology*. 2(1), 23-33.  
DOI: <https://doi.org/10.30564/jhp.v2i1.1905>.